

Neuron, Volume 114

Supplemental information

**A genetically encoded fluorescent sensor
for monitoring spatiotemporal
prostaglandin E2 dynamics *in vivo***

Lei Wang (王蕾), Yini Yang (杨旖旎), Fei Deng (邓飞), Yuqi Yan (鄢羽岐), Huan Wang (王欢), Bohan Li (李柏翰), Jinxia Wan (万金霞), and Yulong Li (李毓龙)

Inventory of Supplemental Information:

Figure S1. Screening of the GRABPGE2 sensor GPCR scaffold and insertion sites, related to Figure 1.

Figure S2. The structure and mutation sites in the PGE2-1.0 sensor, related to Figure 1.

Figure S3. Summary of the change in PGE2-1.0 and PGE2mut fluorescence measured in brain slices in response to IL-1 β , PTZ, and PGE2 perfusion, related to Figure 2.

Figure S4. The expression of PGE2-1.0 does not disrupt the normal physiological temperature response of mice, related to Figure 3.

Figure S5. Using the PGE2-1.0 sensor to detect cortex PGE2 dynamics during voluntary running, related to Figure 3.

Figure S6. The PGE2-1.0 sensor reliably detects seizure-induced changes in PGE2 in vivo, related to Figure 3.

Figure S7. Replotted data from Figure 4D with adjusted scale and statistical analysis, related to Figure 4.

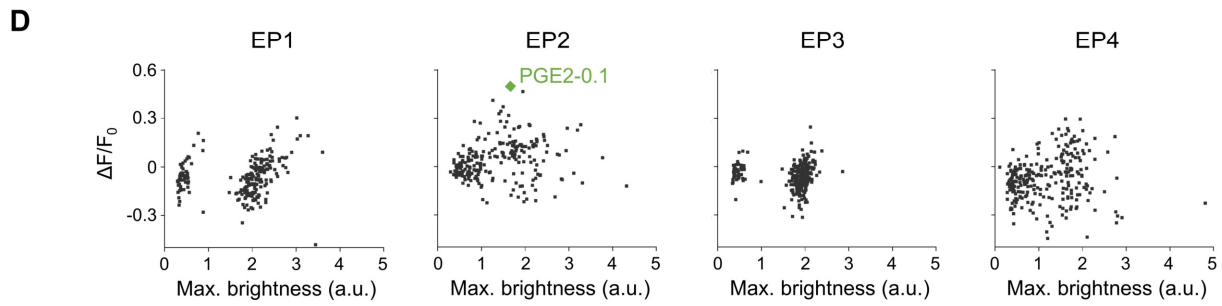
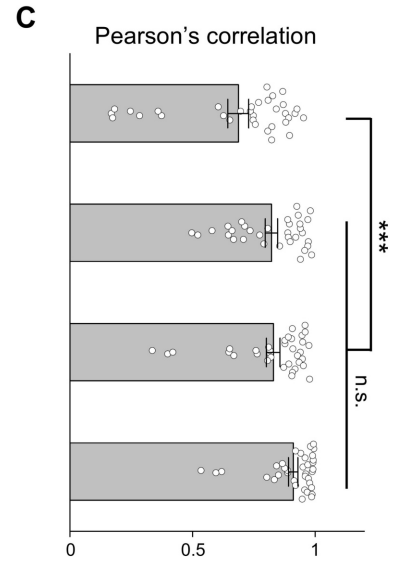
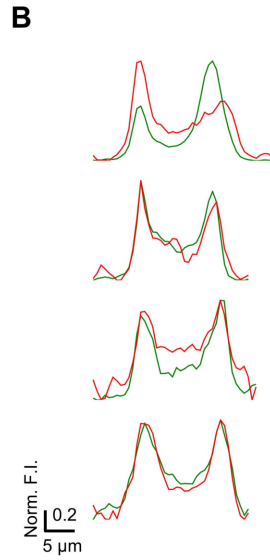
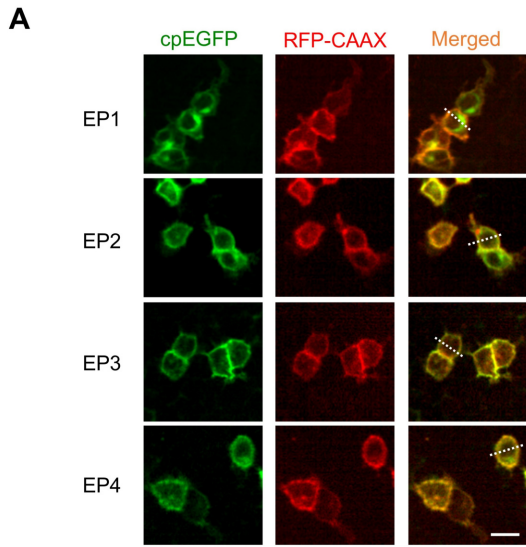


Figure S1. Screening of the GRAB_{PGE2} sensor GPCR scaffold and insertion sites, related to Figure 1.

(A) Representative images of HEK293T cells co-expressing red fluorescent RFP-CAAX (to label the plasma membrane) and prototype GRAB_{PGE2} sensor candidates with cpEGFP inserted in the indicated PGE2 receptor backbones. The dotted lines in the merged images were used to measure the correlation between the green and red fluorescence signals. Scale bar, 20 μ m. **(B)** Line-scan traces of the green (cpEGFP) and red (RFP-CAAX) channels in the images shown in (A). **(C)** Summary of the correlation between the green and red fluorescence signals in order to confirm membrane trafficking of the various GRAB_{PGE2} sensor candidates. n = 33–36 cells/4 wells for EP1–EP4 respectively. **(D)** Peak $\Delta F/F_0$ plotted against maximum brightness for the indicated GRAB_{PGE2} candidates. The candidate with the highest performance (PGE2-0.1) is indicated which was the selected candidate for further optimization. All summary data are presented as the mean \pm the standard error of the mean (SEM). Data were analyzed using one-way ANOVA followed by Tukey's test for multiple comparisons. Where indicated, n.s., not significant ($p > 0.05$), *** $p < 0.001$.

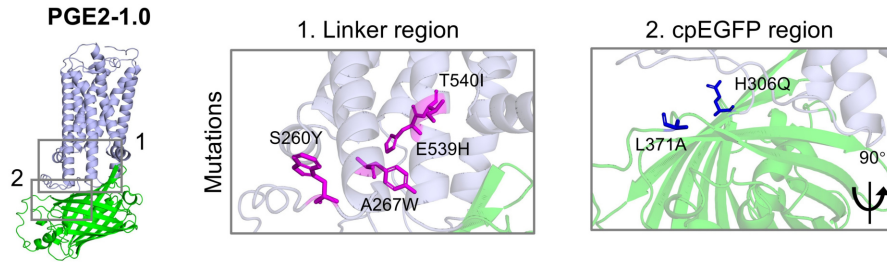
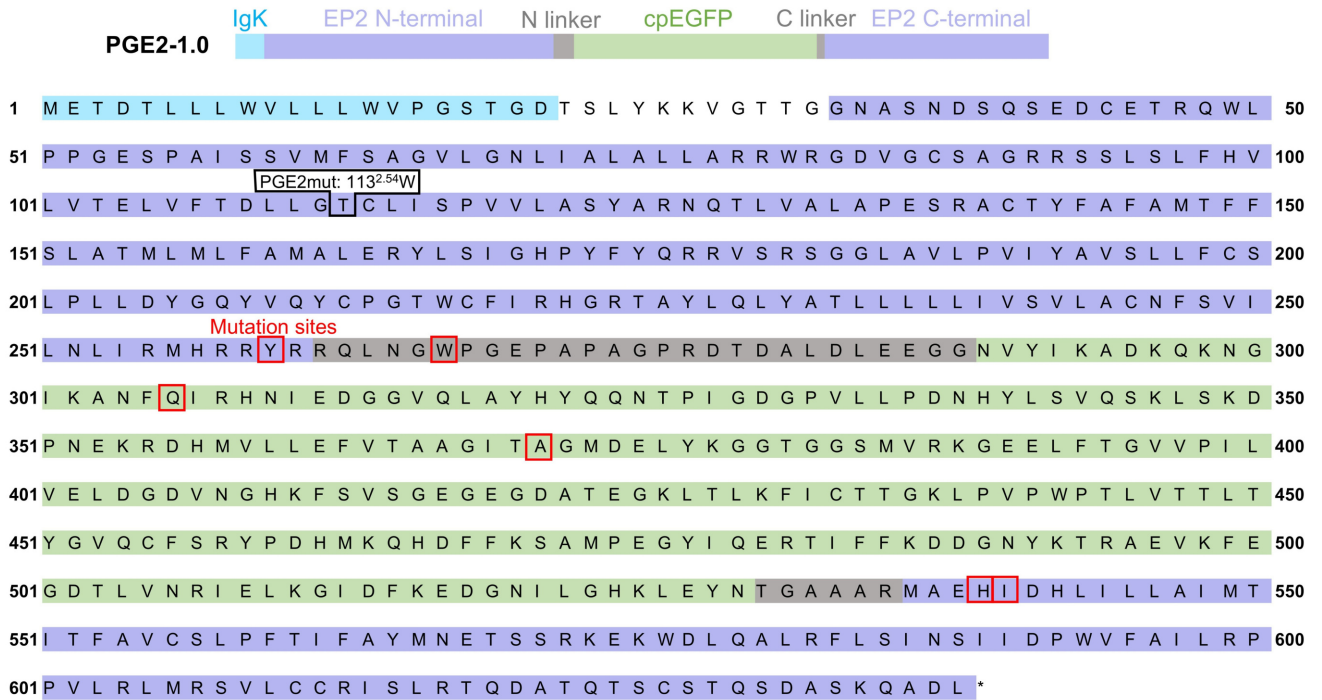
A**B**

Figure S2. The structure and mutation sites in the PGE2-1.0 sensor, related to Figure 1.

(A) Structure of the PGE2-1.0 sensor, with the EP2 GPCR and cpEGFP components shown in purple and green, respectively. The linker and cpEGFP regions in which mutations were introduced to generate PGE2-1.0 are indicated. **(B)** The amino acid sequence of the PGE2-1.0 sensor, with the sensor's domains shown above. The mutation sites for generating the sensor are indicated by red boxes, and the T113^{2.54}W mutation introduced to create the ligand-insensitive PGE2mut version from PGE2-1.0 is indicated by a black box. Note that the amino acid numbering system used here corresponds to the start of the IgK leader sequence.

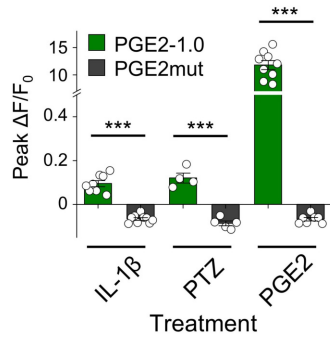
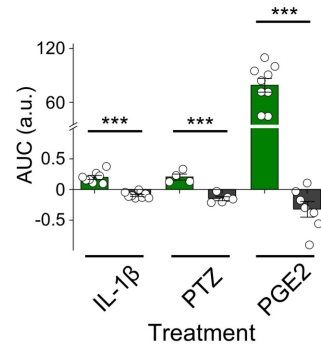
A**B**

Figure S3. Summary of the change in PGE2-1.0 and PGE2mut fluorescence measured in brain slices in response to IL-1 β , PTZ, and PGE2 perfusion, related to Figure 2.

(A) Summary of the peak change in PGE2-1.0 and PGE2mut fluorescence in brain slices in response to IL-1 β (n = 8/6 (8 slices from 6 mice) for PGE2-1.0 sensor, n = 8/3 for PGE2mut), PTZ (n = 4/3 for PGE2-1.0, n = 5/3 for PGE2mut), and PGE2 (n = 9/7 for PGE2-1.0 and n = 7/4 for PGE2mut) perfusion. **(B)** Summary of the area under the curve (AUC) of the change in PGE2-1.0 and PGE2mut fluorescence measured 4 min after perfusing IL-1 β (n = 8/6 for PGE2-1.0, n = 8/4 for PGE2mut) or PTZ (n = 4/3 for PGE2-1.0, n = 5/4 for PGE2mut), and 10 min after perfusing PGE2 (n = 9/7 for PGE2-1.0, n = 7/4 for PGE2mut). All summary data are presented as the mean \pm SEM. Data were analyzed using Student's t-test. Where indicated, ***p < 0.001.

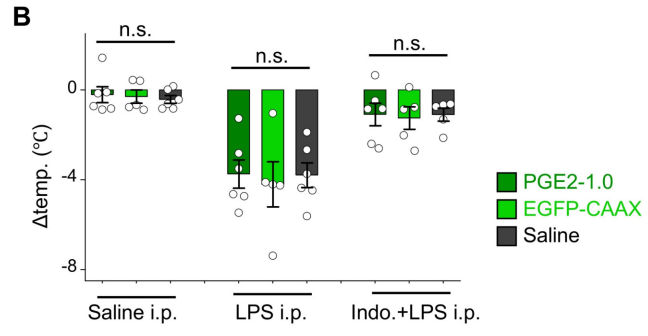
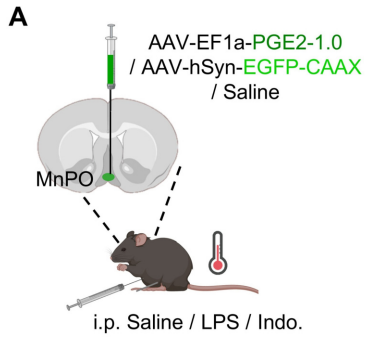


Figure S4. The expression of PGE2-1.0 does not disrupt the normal physiological temperature response of mice, related to Figure 3.

(A) Schematic diagram depicting the strategy for injecting virus; the animal's skin temperature was also recorded during the experiment. **(B)** Summary of the mouse skin temperature change following i.p. injection of saline, 1 mg/kg body weight LPS, or 1 mg/kg body weight LPS following a pre-injection of 15 mg/kg body weight indomethacin. n = 6 mice for the PGE2-1.0 and saline group respectively; n = 5 for the EGFP-CAAX group. All summary data are presented as the mean \pm SEM. Data were analyzed using one-way ANOVA followed by Tukey's test for multiple comparisons. Where indicated, n.s., not significant ($p > 0.05$).

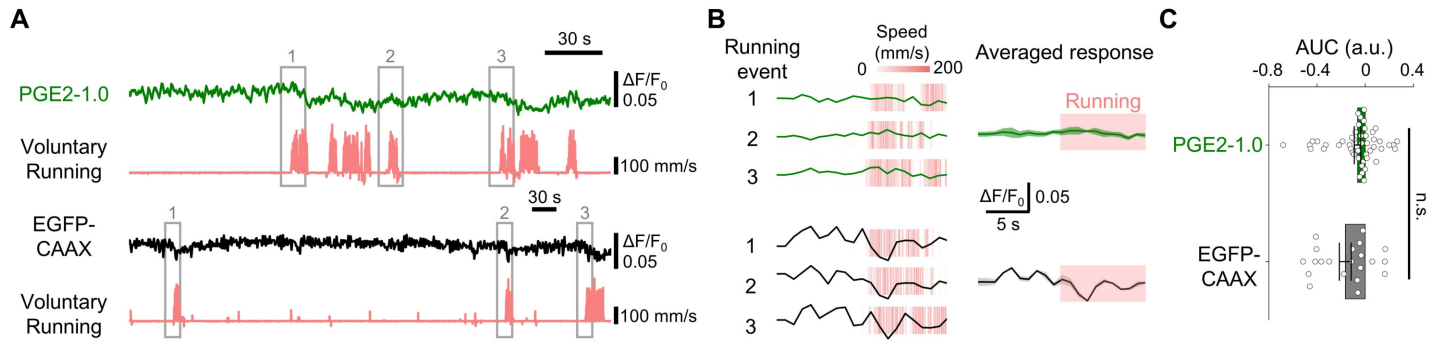


Figure S5. Using the PGE2-1.0 sensor to detect cortex PGE2 dynamics during voluntary running, related to Figure 3.

(A) Example trace of the fluorescence changes of PGE2-1.0 (upper panel) or EGFP-CAAX (lower panel) and simultaneously recorded voluntary running speed. Grey boxes indicate representative running events (1–3) that are expanded in (B). **(B)** (Left) Traces of individual running events. (Right) Averaged fluorescent response aligned to the onset and duration of the running period (indicated by the red shaded box). The upper panel shows PGE2-1.0 responses, and the lower panel shows EGFP-CAAX responses. **(C)** Summary of the area under the curve (AUC) of the change in PGE2-1.0 fluorescence ($n = 49/6$ (49 running events from 6 mice)) and EGFP-CAAX ($n = 21/4$) measured for 10 s after running onset. The summary data are presented as the mean \pm SEM. Data were analyzed using Student's t-test. Where indicated, n.s., not significant ($p > 0.05$).

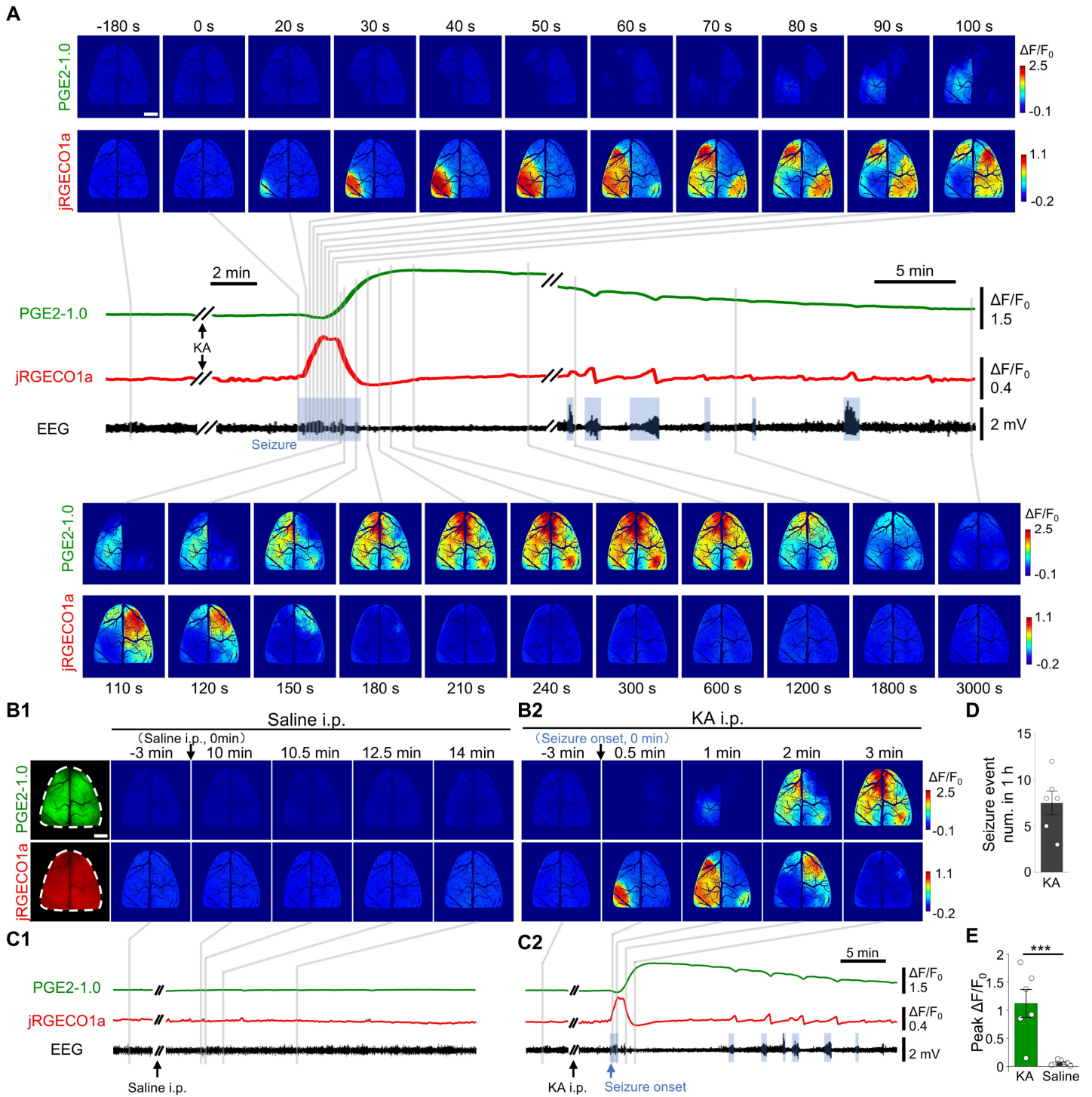
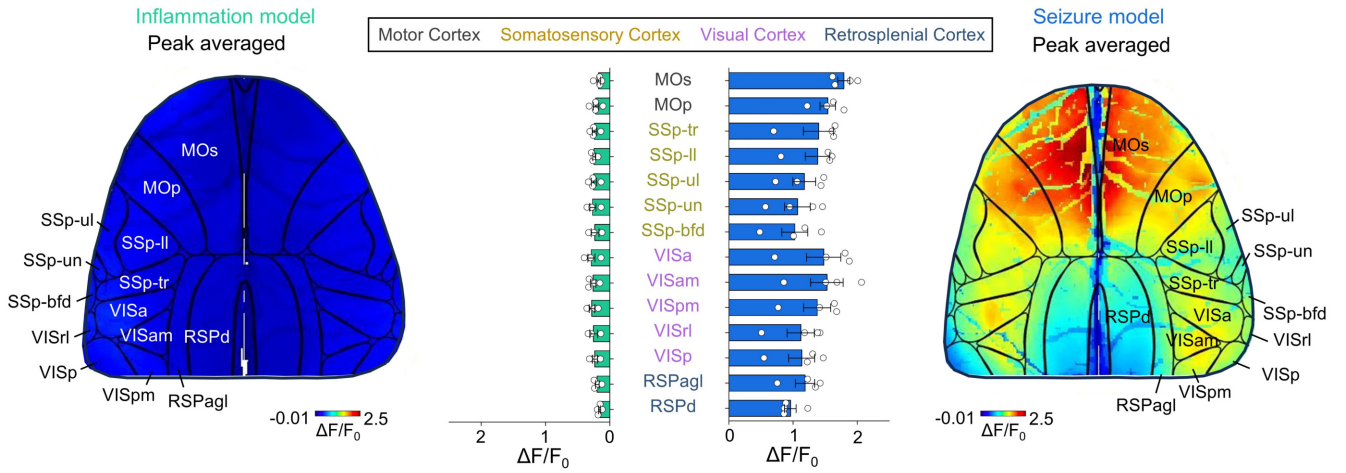


Figure S6. The PGE2-1.0 sensor reliably detects seizure-induced changes in PGE2 *in vivo*, related to Figure 3.

(A) A high-temporal resolution series of representative images and traces of the change in PGE2-1.0 and jRGECO1a fluorescence in response to an i.p. injection of KA (10 mg/kg body weight). Note the different time scales before and after the break. Scale bars, 1 mm. **(B)** Representative images of the change in PGE2-1.0 and jRGECO1a fluorescence in response to an i.p. injection of Saline (B1) and KA (10 mg/kg body weight) (B2). **(C)** The representative traces of the change in PGE2-1.0 and jRGECO1a fluorescence, together with the corresponding EEG signal recorded in Saline (C1) and KA (C2) injected mouse. The blue shaded boxes in the EEG trace indicate epileptic discharges. **(D)** The summary of epileptiform seizure events within 1 h after the first seizure event in KA-induced seizure model. $n = 6$ mice. **(E)** Summary of the peak change in PGE2-1.0 fluorescence measured after injecting KA ($n = 6$ mice, replotted with data from Figure 4C) or Saline ($n = 7$ mice). The summary data are presented as the mean \pm SEM. Data were analyzed using Student's t-test. Where indicated, $***p < 0.001$.

A



B

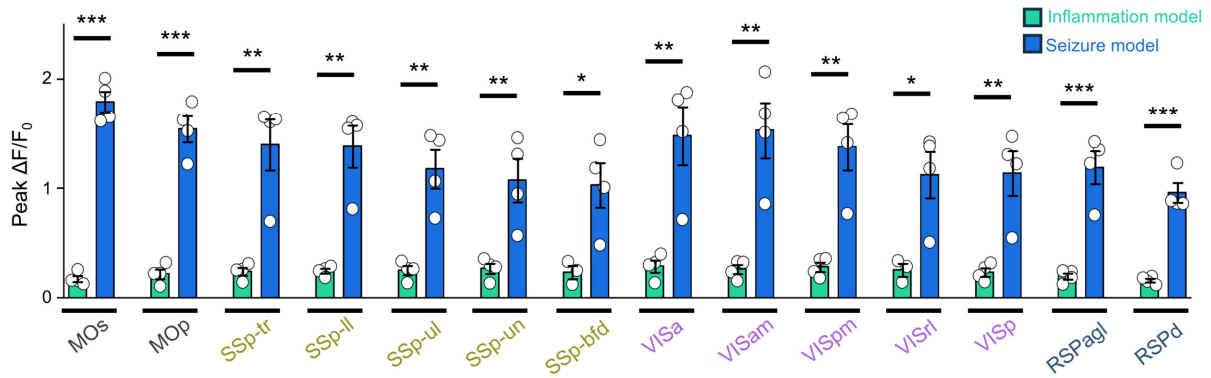


Figure S7. Replotted data from Figure 4D with adjusted scale and statistical analysis, related to Figure 4.

(A) Pseudo-color images depicting the average peak increase in PGE2-1.0 fluorescence measured during inflammation (left) and seizure (right) in same scale (replotted data from Figure 4D). **(B)** Summary of the peak responses measured in the indicated cortical structures with statistical analysis (replotted data from Figure 4D). All summary data are presented as the mean \pm SEM. Data were analyzed using Student's t-test. Where indicated, * $p < 0.05$, ** $p < 0.01$, *** $p < 0.001$.